ROBUST OPTIMIZATION-DIRECTED DESIGN

Nonconvex Optimization and Its Applications

VOLUME 81

ROBUST OPTIMIZATION-DIRECTED DESIGN

Edited by

ANDREW J. KURDILA
University of Florida, Gainesville, Florida

PANOS M. PARDALOS
University of Florida, Gainesville, Florida

MICHAEL ZABARANKIN
Stevens Institute of Technology, Hoboken, New Jersey

Springer

Library of Congress Cataloging-in-Publication Data

Kurdila, Andrew.
Robust optimization-directed design / edited by Andrew J. Kurdila, Panos M. Pardalos, Michael Zabarankin.
p. cm. — (Nonconvex optimization and its applications ; v. 81)
Includes bibliographical references.
ISBN-13: 978-0-387-28263-3
ISBN-10: 0-387-28263-7
ISBN-13: 978-0-387-28654-9 (e-book)
ISBN-10: 0-387-28654-3 (e-book)
1. System theory. 2. Mathematical optimization. 3. Programming (Mathematics) I. Pardalos, P.M. (Panos M.), 1954– II. Zabarankin, Michael, 1974– III. Title. IV. Series.

Q295.K875 2006
003—dc22

2005051643

AMS Subject Classifications: 93C20, 93C95, 93E03, 90C15, 65K10

Printed in the United States of America.

9 8 7 6 5 4 3 2 1 SPIN 11539148

springeronline.com

Contents

Preface

There has been and continues to be a great deal of work on optimization, multi-disciplinary optimal design (MDO), but in spite of the amount of research in MDO, there is a lack of effort in sharing new ideas aimed at addressing some of the practical issues that could lead to more widespread and effective use of optimization as a practical design tool.

Robust design or managing design uncertainties (model uncertainty, parametric uncertainty, etc.) is the unpleasant issue that is crucial in much of the MDO work. There is a lot of work in stochastic optimization, which tries to address some of the issues, and may have some promise for complex, integrated design problems, especially for many practical examples springing from this field. The "Optimization-Directed" expression in the *Robust Optimization-Directed Design* title is meant to suggest that the focus is not on agonizing over whether optimization strategies identify a true global optimum, but on whether they make significant design improvements. Recently, there has been enormous practical interest in strategies for applying optimization tools to the development of robust solutions/designs in

- Aerodynamics: airframes design, modeling and control
- Integration of sensing (laser radars, vision-based systems, millimeter-wave radars) and control
- Cooperative control with poorly modeled uncertainty
- Cascading failures in military and civilian applications
- Multi-mode seekers/sensor fusion
- Data association problems and tracking systems

In April 2004, the University of Florida (UF) Graduate Engineering and Research Center (GERC) and the Center for Agile Autonomous Flight successfully hosted the first conference on Robust Optimization-Directed Design (RODD) in Shalimar, Florida. The RODD meeting brought together outstanding researchers in RODD, researchers working on uncertainty management in complex modeling and simulation problems, stochastic optimization and mathematical modeling experts, in order to understand the state of the art in RODD, and to see what tools and techniques may be available to help in some of the many complex design issues that are arising in the joint Air Force Research Laboratory/Munitions Directorate, Air Force Office of Scientific Research and UF GERC research effort currently being conducted at the new Center for Agile Autonomous Flight. About 30 researchers from government, industry and academia attended the conference and presented their views on robust design, what it means and how it is distinct or related to other fields of research. This book contains refereed papers summarizing the participants' research in uncertainty modelling, robust design, optimal control and stochastic optimization.

We would like to take the opportunity to thank the authors of the papers, the UF Center for Agile Autonomous Flight for financial support, Dr. Marc Jacobs for the help in organizing the conference, the anonymous referees and Springer Publisher for making the publication of this volume possible.

Andrew J. Kurdila, Panos M. Pardalos and Michael Zabarankin
April 2005

Everything flows, nothing stands still. No man can cross the same river twice, because neither the man nor the river are the same.

Heraclitus, 535–475 B.C.

1

A Multigrid Approach to Optimal Control Computations for Navier-Stokes Flows

E. Aulisa[1] and S. Manservisi[2]

[1] DIENCA
University of Bologna
Via dei colli 16
Bologna, Italy
[2] Departments of Mathematics and Statistics
Texas Tech University
Lubbock Texas 79409-1042
smanserv@math.ttu.edu

Summary. Optimal control computations with boundary controls are presented by using a new multigrid approach for reliable and robust optimization. The multigrid implementation is based on a local Vanka-type solver for the Navier-Stokes and the adjoint system. The solution is achieved by solving and relaxing element by element the optimal control problem which is formulated by using an embedded domain approach. Numerical tests for steady and unsteady solutions are presented to prove the effectiveness and robustness of the method for flow matching and tracking.

Key words: optimal control, Navier-Stokes equations, Multigrid methods, Vanka-type solvers

1.1 Introduction

Optimal boundary control problems associated with the Navier-Stokes equations have a wide and important range of applications. Aerodynamic and hydrodynamic problems such as the design of cars, airplanes, and jet engines provide a few settings. Despite the fact that this field has been extensively studied, determining the optimal control for a system governed by the Navier-Stokes equations is still a difficult and time consuming task. The optimal control of the Navier-Stokes equations shows many challenges and has been considered by numerous authors, e.g., [1], [4], [6], [7], [8], [11], [12], [13], [16], [19] and [24]. However in many of these papers the formulation is not suitable for applications since the function spaces proposed for the solution may not allow accurate finite element implementations or may not allow a suitable numerical form for the optimality system.

In this paper, we study a class of optimal flow control problems and its multigrid implementation for which the fluid motion is controlled by velocity forcing, i.e., injection or suction, along a portion of the boundary, and the cost or objective functional is a measure of the discrepancy between the flow velocity and a given target velocity. We consider the two-dimensional incompressible flow of a viscous fluid on the do-

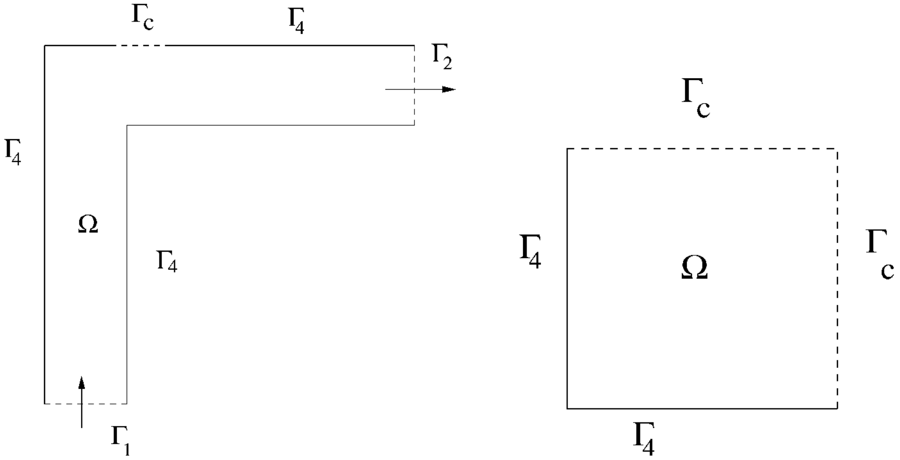

Fig. 1.1. Flow domain: Γ_1 inflow, Γ_2 outflow and Γ_c controlled boundary.

main Ω with boundary Γ. For example a typical L-shaped channel domain is shown in Figure 1.1 on the left and a square domain on the right with boundary control over Γ_c. The velocity $\mathbf{u}$ and the pressure p satisfy the Navier-Stokes system

$$\frac{\partial \mathbf{u}}{\partial t} + (\mathbf{u} \cdot \nabla)\mathbf{u} = -\nabla p + \nu \triangle \mathbf{u} + \mathbf{f} \qquad \text{in } \Omega \tag{1.1}$$

$$\nabla \cdot \mathbf{u} = 0 \qquad \text{in } \Omega \tag{1.2}$$

along with the Dirichlet boundary conditions

$$\mathbf{u} = \mathbf{g} = \begin{cases} \mathbf{g}_1 & \text{on } \Gamma_1 \\ \mathbf{g}_2 & \text{on } \Gamma_2 \\ \mathbf{g}_c & \text{on } \Gamma_c \\ \mathbf{0} & \text{on } \Gamma_4 \end{cases} \tag{1.3}$$

where $\mathbf{f}$ is the given body force. In (1.3), ν denotes the inverse of the Reynolds number whenever the variables are appropriately nondimensionalized. The vectors $\mathbf{g}_1$ and $\mathbf{g}_2$ are the given velocities at the inflow Γ_1 and outflow Γ_2 of the channel, respectively. Along the boundary Γ_4 of the channel the velocity vanishes. The velocity at the outflow Γ_2 may be specified by using Neumann boundary control. The function $\mathbf{g}$ must satisfy the compatibility condition

$$\int_\Gamma \mathbf{g} \cdot \mathbf{n} \, ds = 0 \,, \tag{1.4}$$

where $\mathbf{n}$ is the unit normal vector along the surface Γ.

There is a substantial literature discussing the set of all possible boundary controls. Clearly, the function $\mathbf{g}_c$ must belong to $H^{1/2}(\Gamma_c)$, the Sobolev space of order $1/2$. However $H^{1/2}(\Gamma_c)$ or $H^1(\Gamma_c)$ may not be sufficient to enable one to explicitly derive a first-order necessary condition. Thus in general the set of all admissible controls $\mathbf{g}$ must be restricted to more regular spaces, namely, to belong to $H^{3/2}(\Gamma_c)$. In this paper we define a set of allowable boundary controls by using distributed control on the extended domain. Let $\widehat{\Omega}$ and $\widehat{\Gamma}$ be the extended domain and boundary respectively where $\widehat{\Gamma}$ contains $\Gamma - \Gamma_c$. We define $\widehat{f}$ the extended force function such that $\widehat{f} = \mathbf{f}$ on Ω. Then, the set of admissible boundary controls can be taken as the set of all $\mathbf{g}_c \in H^{3/2}(\Gamma_c)$ such that $\mathbf{g}_c$ is the trace of the extended solution $\widehat{u}$ of (1.3) over $\widehat{\Omega}$ with distributed control $\widehat{f}$.

One could examine several practical objective functionals for determining the shape of the boundary, e.g., the reduction of the drag due to viscosity or the identification of the velocity at a fixed vertical slit downstream. To fix ideas, we focus on the minimization of the cost functional

$$\mathcal{J} = \int_{\Omega_1} |\mathbf{u} - \hat{u}|^2 \, d\mathbf{x} + \frac{\beta}{2} \int_{\widehat{\Omega} - \Omega} |\hat{f}|^2 \, d\mathbf{x} \,, \tag{1.5}$$

for stationary matching or

$$\begin{aligned} \mathcal{J} = \int_0^T \int_{\Omega_1} |\mathbf{u} - \mathbf{U}|^2 \, d\mathbf{x} + \frac{\alpha}{2} \int_{\Omega} |\mathbf{u}(T) - \mathbf{U}(T)|^2 \, d\mathbf{x} \\ + \frac{\beta}{2} \int_0^T \int_{\widehat{\Omega} - \Omega} |\hat{f}|^2 \, d\mathbf{x} \,, \end{aligned} \tag{1.6}$$

for time dependent control. The velocity field $\mathbf{U}$ is the desired velocity field defined on $\Omega_1 \subset \Omega$, α and β are nonnegative constants. Formally speaking, by using this formulation the boundary control problem is reduced to solving a distributed control problem over the $\hat{\Omega} - \Omega$ domain.

In literature the standard steady optimal control problem is formulated by using the following functional (see for example [1; 13])

$$\mathcal{J} = \frac{\alpha}{2} \int_{\Omega} |\mathbf{u} - \mathbf{U}|^2 \, d\mathbf{x} + \frac{\beta}{2} \int_{\Gamma_c} (|\mathbf{g}|^2 + \beta_1 |\mathbf{g}_x|^2) \, d\mathbf{x}, \tag{1.7}$$

where the minimization of the first term involving $(\mathbf{u} - \mathbf{U})$ is the real goal of the velocity matching problem and the other terms have been introduced in order to bound the control function and prove the existence of the solution of the optimal control problem and the optimality system. We may effectively limit the size of the control and prove the existence of the first order necessary condition for optimality through an appropriate choice of the positive coefficients β and β_1 but the optimal control based on this admissible set of solutions and the choice of β and β_1 is not very friendly from the numerical point of view and it turns out to be a very difficult task if injection or suction boundary velocity is required to satisfy the integral constraint (1.4).

In this paper the functional (1.5) is used and the optimal boundary control is obtained as the trace of the solution over the extended domain. Computations of the optimality system are performed by using a new multigrid approach. The implementation is based on a local Vanka-type solver for the Navier-Stokes and the adjoint system where solution is achieved by solving and relaxing element by element the optimal control problem. The multigrid smoother operator is constructed directly from the optimal control formulation and requires the iterative exact solution of the optimality system over a limited number of unknowns. Numerical tests for steady and unsteady solutions are presented. Unsteady optimal control is presented in the form of a time piecewise optimal control problem which proves to be a very effective and robust method for flow tracking. Also in this multigrid approach the solution of the unsteady optimal problem is achieved by solving iteratively several optimal problems over all the time steps but over a limited number of degrees of freedom in space. This allows us to solve the couple time-space optimality system exactly over a sufficient large number of time steps and enhances enormously the capability of solving boundary optimal control problems for complex geometries.

1.2 The Stationary Boundary Control Problem

We denote by $H^s(\mathcal{O})$, $s \in \mathbb{R}$, the standard Sobolev space of order s with respect to the set $\mathcal{O}$, which is either the flow domain Ω, or its boundary Γ, or part of its boundary. Whenever m is a nonnegative integer, the inner product over $H^m(\mathcal{O})$ is denoted by $(f,g)_m$ and (f,g) denotes the inner product over $H^0(\mathcal{O}) = L^2(\mathcal{O})$. Hence, we associate with $H^m(\mathcal{O})$ its natural norm $\|f\|_{m,\mathcal{O}} = \sqrt{(f,f)_m}$. Whenever possible, we will neglect the domain label in the norm.

For vector-valued functions and spaces, we use boldface notation. For example, $\mathbf{H}^s(\Omega) = [H^s(\Omega)]^n$ denotes the space of $\mathbb{R}^n$-valued functions such that each component belongs to $H^s(\Omega)$. Of special interest is the space

$$\mathbf{H}^1(\Omega) = \left\{ v_j \in L^2(\Omega) \;\middle|\; \frac{\partial v_j}{\partial x_k} \in L^2(\Omega) \quad \text{for } j,k = 1,2 \right\},$$

equipped with the norm $\|\mathbf{v}\|_1 = (\sum_{k=1}^{2} \|v_k\|_1^2)^{1/2}$.

For $\Gamma_s \subset \Gamma$ with nonzero measure, we also consider the subspace

$$\mathbf{H}^1_{\Gamma_s}(\Omega) = \{ \mathbf{v} \in \mathbf{H}^1(\Omega) \mid \mathbf{v} = \mathbf{0} \quad \text{on } \Gamma_s \}.$$

Also, we write $\mathbf{H}^1_0(\Omega) = \mathbf{H}^1_\Gamma(\Omega)$. For any $\mathbf{v} \in \mathbf{H}^1(\Omega)$, we write $\|\nabla \mathbf{v}\|$ for the seminorm. Let $(\mathbf{H}^1_{\Gamma_s})^*$ denote the dual space of $\mathbf{H}^1_{\Gamma_s}$. Note that $(\mathbf{H}^1_{\Gamma_s})^*$ is a subspace of $\mathbf{H}^{-1}(\Omega)$, where the latter is the dual space of $\mathbf{H}^1_0(\Omega)$. The duality pairing between $\mathbf{H}^{-1}(\Omega)$ and $\mathbf{H}^1_0(\Omega)$ is denoted by $\langle \cdot, \cdot \rangle$.

Let g be an element of $\mathbf{H}^{1/2}(\Gamma)$. It is well known that $\mathbf{H}^{1/2}(\Gamma)$ is a Hilbert space with norm

$$\|\mathbf{g}\|_{1/2,\Gamma} = \inf_{\mathbf{v} \in \mathbf{H}^1(\Omega);\, \gamma_\Gamma \mathbf{v} = \mathbf{g}} \|\mathbf{v}\|_1 ,$$

where γ_Γ denotes the trace mapping $\gamma_\Gamma : \mathbf{H}^1(\Omega) \to \mathbf{H}^{1/2}(\Gamma)$. We let $(\mathbf{H}^{1/2}(\Gamma))^*$ denote the dual space of $\mathbf{H}^{1/2}(\Gamma)$ and $\langle \cdot, \cdot \rangle_\Gamma$ denote the duality pairing between $(\mathbf{H}^{1/2}(\Gamma))^*$ and $\mathbf{H}^{1/2}(\Gamma)$. Let Γ_s be a smooth subset of Γ. Then, the trace mapping $\gamma_{\Gamma_s} : \mathbf{H}^1(\Omega) \to \mathbf{H}^{1/2}(\Gamma_s)$ is well defined and $\mathbf{H}^{1/2}(\Gamma_s) = \gamma_{\Gamma_s}(\mathbf{H}^1(\Omega))$.

Since the pressure is only determined up to an additive constant by the Navier-Stokes system with velocity boundary conditions, we define the space of square integrable functions having zero mean over Ω as

$$L_0^2(\Omega) = \{ p \in L^2(\Omega) \mid \int_\Omega p \, d\mathbf{x} = 0 \} .$$

In order to define a weak form of the Navier-Stokes equations, we introduce the continuous bilinear forms

$$a(\mathbf{u}, \mathbf{v}) = 2\nu \sum_{i,j=1}^{2} \int_\Omega D_{ij}(\mathbf{u}) \, D_{ij}(\mathbf{v}) \, d\mathbf{x} \qquad \forall \, \mathbf{u}, \mathbf{v} \in \mathbf{H}^1(\Omega) \tag{1.8}$$

and

$$b(\mathbf{v}, q) = - \int_\Omega q \, \nabla \cdot \mathbf{v} \, d\mathbf{x} \quad \forall q \in L_0^2(\Omega) , \quad \forall \mathbf{v} \in \mathbf{H}^1(\Omega) \tag{1.9}$$

and the trilinear form

$$\begin{aligned} c(\mathbf{w}; \mathbf{u}, \mathbf{v}) &= \int_\Omega \mathbf{w} \cdot \nabla \mathbf{u} \cdot \mathbf{v} \, d\mathbf{x} \\ &= \sum_{i,j=1}^{2} \int_\Omega w_j \left(\frac{\partial u_i}{\partial x_j} \right) v_i \, d\mathbf{x}, \quad \forall \, \mathbf{w}, \mathbf{u}, \mathbf{v} \in \mathbf{H}^1(\Omega) . \end{aligned} \tag{1.10}$$

Obviously, $a(\cdot, \cdot)$ is a continuous bilinear form on $\mathbf{H}^1(\Omega) \times \mathbf{H}^1(\Omega)$, $b(\cdot, \cdot)$ is a continuous bilinear form on $\mathbf{H}^1(\Omega) \times L_0^2(\Omega)$ and $c(\cdot; \cdot, \cdot)$ is a continuous trilinear form on $\mathbf{H}^1(\Omega) \times \mathbf{H}^1(\Omega) \times \mathbf{H}^1(\Omega)$. For details concerning the function spaces we have introduced, one may consult [2; 25] and for details about the bilinear and trilinear forms and their properties, one may consult [9; 25].

We now formulate the mathematical model of the optimal boundary control problem. Let $\widehat{\Omega}$ be an extended domain and $\widehat{\Gamma}$ be the corresponding boundary. If Γ_c is the part of the boundary where we apply the control we assume that $\Gamma - \Gamma_c$ is a subset of $\widehat{\Gamma}$, namely only the controlled part of the boundary lies inside the extended domain $\widehat{\Omega}$. In the rest of the paper we denote by u the restriction to Ω of the function $\widehat{u}$ defined over the domain $\widehat{\Omega}$ and vice-versa. Some properties of an extension or a solenoidal extension of a function defined in Ω can be found in [2].

The optimal boundary control problem can then be stated by using the extended domain $\widehat{\Omega}$ and the distributed extended force $\widehat{f}$ in the following way:

find $\widehat{f} \in \mathbf{L}^2(\widehat{\Omega} - \Omega)$ *such that* $(\widehat{u}, \widehat{p}, \widehat{\tau})$ *minimizes the functional*

$$\mathcal{J} = \int_{\Omega_1} |\mathbf{u} - \mathbf{U}|^2 \, d\mathbf{x} + \frac{\beta}{2} \int_{\Omega - \hat{\Omega}} |\hat{f}|^2 \, d\mathbf{x} , \tag{1.11}$$

and satisfies

$$\begin{cases} a(\widehat{u},\widehat{v}) + c(\widehat{u};\widehat{u},\widehat{v}) + \langle \widehat{\tau},\widehat{v}\rangle_{\widehat{\Gamma}} + b(\widehat{v},p) \\ \qquad\qquad = \langle \widehat{f},\widehat{v}\rangle, \quad \forall \widehat{v} \in \mathbf{H}^1(\widehat{\Omega}) \\ b(\widehat{u},\widehat{q}) = 0, \quad \forall \widehat{q} \in L^2_0(\widehat{\Omega}) \\ \langle \widehat{u},\widehat{s}\rangle_{\widehat{\Gamma}} \;=\; \langle \widehat{g},\widehat{s}\rangle_{\widehat{\Gamma}}, \quad \forall \widehat{s} \in \mathbf{H}^{-1/2}(\widehat{\Gamma}) \end{cases} \tag{1.12}$$

with $\widehat{f} = \mathbf{f}$ over Ω. The domain Ω_1 is the part of the domain over which the matching is desired. The corresponding boundary control $\mathbf{g}_c \in \mathbf{H}^{3/2}(\Gamma_c)$ can be found after the solution of the above optimal control problem as the trace of the extended solution $\widehat{u}$ over Γ_c. We note that the boundary control $\mathbf{g}_c$ automatically satisfies the compatibility condition (1.4). Existence and uniqueness results for solutions of the system (1.12) are contained in [9; 25]. Note that solutions of (1.12) exists for any value of the Reynolds number. However the uniqueness can be guaranteed only for "large enough" values of ν or for "small enough" data $\mathbf{f}$ and $\mathbf{g}$. The admissible set of states and controls is given by

$$\begin{aligned} \mathcal{A}_{ad} = \{(\mathbf{u},p,\widehat{f},\mathbf{g}_c) &\in \mathbf{H}^1(\Omega) \times L^2_0(\Omega) \times \mathbf{L}^2_0(\widehat{\Omega}) \times \mathbf{H}^{3/2}(\Gamma_c) \\ &\text{with } \mathbf{g}_c = \gamma_{\Gamma_c}\widehat{u} \;\text{ and }\; \widehat{f} = \mathbf{f} \;\text{ over }\; \Omega \\ &\text{such that } \mathcal{J}(\mathbf{u},\widehat{f}) < \infty \;\text{ and }\; (\widehat{u},\widehat{p}) \;\text{ satisfies (1.12)}\}\,. \end{aligned}$$

The existence of optimal solutions in this admissible set can be studied by using standard techniques (see for example [1; 8; 11; 12; 13]). Following this approach it is possible to show that optimal control solutions must satisfy a first-order necessary condition. They must satisfy the following Navier-Stokes system

$$\begin{cases} \nu a(\widehat{u},\widehat{v}) + c(\widehat{u};\widehat{u},\widehat{v}) + b(\widehat{v},\widehat{p}) = \langle \widehat{f},\widehat{v}\rangle, \quad \forall \widehat{v} \in \mathbf{H}^1_{\widehat{\Gamma}-\Gamma_2}(\widehat{\Omega}) \\ b(\widehat{u},\widehat{q}) = 0, \quad \forall \widehat{q} \in L^2_0(\widehat{\Omega}) \\ \langle \widehat{u},\widehat{s}\rangle_{\widehat{\Gamma}-\Gamma_2} = \langle \widehat{g},\widehat{s}\rangle_{\widehat{\Gamma}-\Gamma_2}, \qquad \forall \widehat{s} \in \mathbf{H}^{-1/2}(\widehat{\Gamma}) \end{cases} \tag{1.13}$$

and the adjoint system

$$\begin{cases} \nu a(\widehat{w},\widehat{v}) + c(\widehat{w};\widehat{u},\widehat{v}) + c(\widehat{u};\widehat{w},\widehat{v}) + b(\widehat{v},\widehat{\sigma}) \\ \qquad\qquad = \displaystyle\int_{\Omega_1} (\mathbf{u}-\mathbf{U})\,\widehat{v}\,d\mathbf{x}, \quad \forall \widehat{v} \in \mathbf{H}^1_{\widehat{\Gamma}-\Gamma_2}(\widehat{\Omega}) \\ b(\widehat{w},\widehat{q}) = 0, \quad \forall \widehat{q} \in L^2_0(\widehat{\Omega}) \\ \langle \widehat{w},\widehat{s}\rangle_{\widehat{\Gamma}-\Gamma_2} = 0, \qquad \forall \widehat{s} \in \mathbf{H}^{-1/2}(\widehat{\Gamma}) \end{cases} \tag{1.14}$$

with

$$\mathbf{g}_c = \gamma_{\Gamma_c}\widehat{u}, \tag{1.15}$$

and $\widehat{f} = \mathbf{f}$ over Ω and $\widehat{f} = \widehat{w}/\beta$ over $\widehat{\Omega} - \Omega$. Γ_2 is the part of the boundary where homogeneous Neumann boundary conditions (outflow) are imposed. The optimality system for the boundary control is reduced to a distributed optimal control problem which requires much less computational resources than other boundary control formulations. In this case there are no regularization parameters involved with the exception of β and the compatibility condition is automatically satisfied. The tangential control can be numerically achieved by using non-embedded techniques but in all these formulations the compatibility constraint is a limit to the feasibility of the normal boundary control. The normal boundary control must obey to this integral constraint reducing enormously the possibility to achieve accurate and fast numerical solutions of the necessary optimal control system with non-embedded techniques.

1.2.1 Numerical Computation of the Boundary Control Problem

The optimal boundary control problem can be solved by using a multigrid approach and the multigrid smoothing operator for each grid level can be derived directly from the optimal control problem. There is a vast class of smoothing operators for multigrid methods but we are interested in the class of Vanka-type solvers. In this class of solvers, which are well known for solving Navier-Stokes equations, the iterative solution is achieved by solving several exact systems involving blocks of variables. In particular we use the close relationship between this class of solvers and the class of solvers arising from saddle point or minimization problems

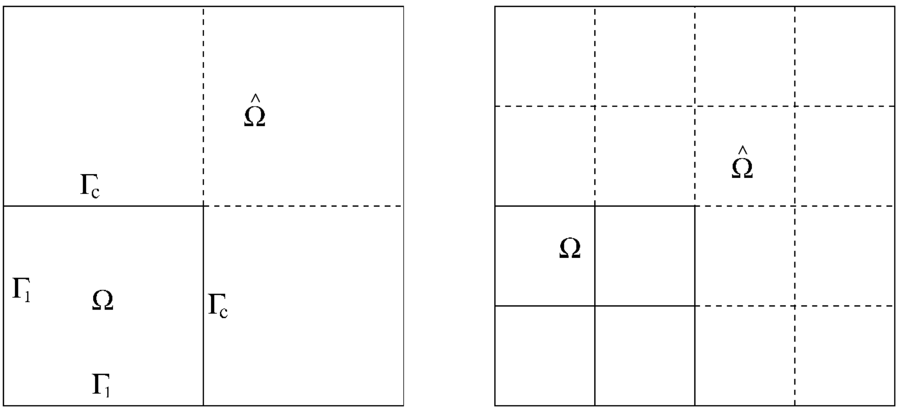

Fig. 1.2. Domain Ω and extended domain $\widehat{\Omega}$ at grid level l_0 (on the left) and at the grid level l_1 (on the right).

which allows us to use conforming isoparametric finite elements.

Let $\widehat{\Omega}_h$ be the square geometry described in Figure 1.2 on the left. Now, by starting at the multigrid coarse level l_0 we subdivide $\widehat{\Omega}_h$ into triangles or rectangles by unstructured families of meshes T_h^{i,l_0}. Based on the simple element midpoint refinement different multigrid levels can be built to reach a complete unstructured mesh $T_h^{i,l}$ for finite element over the entire domain Ω_h at the top finest multigrid level l_{n_l}. For example in Figure 1.2 on the right the mesh obtained by simple midpoint refinement is shown at the grid level l_1 (on the right).

We introduce the approximation spaces $\mathbf{X}_{h_l} \subset \mathbf{H}^1(\widehat{\Omega})$ and $S_{h_l} \subset L^2(\widehat{\Omega})$ for the extended velocity and pressure respectively at the multigrid level l. The approximate function obeys to the standard approximation properties including the LBB-condition. Let $P_{h_l} = X_{h_l}|_{\partial\widehat{\Omega}}$, i.e., P_{h_l} consists of all the restrictions, to the boundary $\partial\widehat{\Omega}$, of functions belonging to X_{h_l}. For all choices of conforming finite element space X_h we then have that $P_{h_l} \subset H^{-\frac{1}{2}}(\partial\widehat{\Omega})$. See [12] for details concerning these approximation spaces. The extended velocity and pressure fields $(\widehat{u}_{h_l}, \widehat{p}_{h_l}) \in \mathbf{X}_{h_l}(\widehat{\Omega}_h) \times S_{h_l}(\widehat{\Omega}_h)$ at the level l satisfy the Navier-Stokes equations

$$\begin{cases} a(\widehat{u}_{h_l}, \widehat{v}_{h_l}) + c(\widehat{u}_{h_l}; \widehat{u}_{h_l}, \widehat{v}_{h_l}) + b(\widehat{v}_{h_l}, \widehat{p}_{h_l}) = \langle \widehat{f}_{h_l}, \widehat{v}_{h_l} \rangle \\ \qquad \forall \widehat{v}_{h_l} \in \mathbf{X}_{h_l}(\widehat{\Omega}_h) \cap \mathbf{H}^1_{\widehat{\Gamma}_h - \Gamma_{2h}}(\widehat{\Omega}_h) \\ b(\widehat{u}_{h_l}, \widehat{r}_{h_l}) = 0, \quad \forall \widehat{r}_{h_l} \in S_{h_l}(\widehat{\Omega}_h) \\ \langle \widehat{u}_{h_l}, \widehat{s}_{h_l} \rangle_{\widehat{\Gamma}_h - \Gamma_{2h}} = \langle \mathbf{g}, \widehat{s}_{h_l} \rangle_{\widehat{\Gamma}_h - \Gamma_{2h}}, \quad \forall \widehat{s}_{h_l} \in \mathbf{P}_{h_l}(\widehat{\Gamma}_h) \end{cases} \tag{1.16}$$

and the adjoint

$$\begin{cases} a(\widehat{w}_{h_l}, \widehat{v}_{h_l}) + c(\widehat{w}_{h_l}; \widehat{u}_{h_l}, \widehat{v}_{h_l}) + c(\widehat{u}_{h_l}; \widehat{w}_{h_l}, \widehat{v}_{h_l}) + b(\widehat{v}_{h_l}, \widehat{\sigma}_{h_l}) \\ \quad = \int_{\Omega_1} (\mathbf{u}_{h_l} - \mathbf{U}) \cdot \widehat{v}_{h_l} \, d\mathbf{x}, \quad \forall \widehat{v}_{h_l} \in \mathbf{X}_{h_l}(\widehat{\Omega}_h) \cap \mathbf{H}^1_{\widehat{\Gamma}_h - \Gamma_{2h}}(\widehat{\Omega}_h) \\ b(\widehat{w}_{h_l}, \widehat{q}_{h_l}) = 0, \quad \forall \widehat{q}_{h_l} \in S_{h_l}(\widehat{\Omega}_h) \\ \langle \widehat{w}_{h_l}, \widehat{s}_{h_l} \rangle_{\widehat{\Gamma_h} - \Gamma_{2h}} = 0, \qquad \forall \widehat{s}_{h_l} \in \mathbf{P}_{h_l}(\widehat{\Gamma}_h) \end{cases} \tag{1.17}$$

with

$$\mathbf{g}_{ch_l} = \gamma_{\Gamma_c} \widehat{u}_{h_l} \tag{1.18}$$

and $\widehat{f}_{h_l} = \mathbf{f}_h$ over Ω_{h_l} and $\widehat{f}_{h_l} = \widehat{w}_{h_l}/\beta$ over $\widehat{\Omega}_{h_l} - \Omega_{h_l}$. Existence and uniqueness results for finite element solutions of (1.16) are well known; see, e.g., [9; 11].

The unique representations of $\widehat{u}_{h_l}$,$\widehat{w}_{h_l}$ and $\widehat{p}_{h_l}$, $\widehat{\sigma}_{h_l}$ as a function of the nodal point values $\widehat{u}_l(k_1)$, $\widehat{w}_l(k_1)$ and $\widehat{p}_l(k_2)$, $\widehat{\sigma}_l(k_2)$ ($k_1 = 1, 2, ...nvt$ with $nvt =$ number of vertex velocity points and $k_2 = 1, 2, ...npt$ with $npt =$ number of vertex pressure points) define the finite element isomorphisms $\Phi_l : U_l \to X_{hl}$, $\Phi_l^+ : W_l \to X_{hl}$, $\Psi_l : \Pi_l \to S_{hl}$ $\Psi_l^+ : \Sigma_l \to S_{hl}$ between the vector spaces U_l, W_l, Π_l, Σ_l of nvt-dimension and npt-dimension vectors and the finite element spaces X_{h_l}, S_{h_l}.

At the level l we introduce the corresponding finite element matrices A_l, B_l and $C_l(\widehat{u}_{h_l})$ for the discrete Navier-Stokes operators a, b, c defined by (1.8)–(1.10) respectively. Their corresponding finite element matrices for the adjoint operators are denoted by A_l^+, B_l^+ and $C_l^+(\widehat{u}_{h_l})$. The Navier-Stokes/adjoint coupled terms are denoted by H_l and G_l. Now the problem (1.16) is equivalent to

$$\begin{pmatrix} A_l + C_l & B_l{}^T & H_l & 0 \\ B_l & 0 & 0 & 0 \\ G_l & 0 & A_l^+ + C_l^+ & (B_l^+)^T \\ 0 & 0 & B_l^+ & 0 \end{pmatrix} \begin{pmatrix} \widehat{u}_{h_l,n} \\ \widehat{p}_{h_l,n} \\ \widehat{w}_{h_l,n} \\ \widehat{\sigma}_{h_l,n} \end{pmatrix} = \begin{pmatrix} \widehat{F}_{h_l} \\ 0 \\ \widehat{R}_{h_l} \\ 0 \end{pmatrix} \tag{1.19}$$

at the multigrid level l. In the vector spaces U_l, W_l, Π_l and Σ_l we use the usual Euclidean norms which can be proved equivalent to the norms introduced to the corresponding finite element approximation spaces (see [5; 17] for details).

Essential elements of a multigrid algorithm are the velocity and pressure prolongation maps

$$P_{l,l-1}(u) : U_{l-1} \to U_l,$$
$$P_{l,l-1}(p) : \Pi_{l-1} \to \Pi_l,$$

and the velocity and restriction operators

$$R_{l-1,l}(u) = P^*_{l,l-1}(u) : U_l \to U_{l-1},$$
$$R_{l-1,l}(u) = P^*_{l,l-1}(u) : \Pi_l \to \Pi_{l-1}.$$

Since we would like to use conforming Taylor-Hood finite element approximation spaces we have the nested finite element hierarchies $X_{h_0} \subset X_{h_1} \subset ... \subset X_{h_l}$ and $S_{h_0} \subset S_{h_1} \subset ... \subset S_{h_l}$ and the canonical prolongation maps $P_{l,l-1}(u)$, $P_{l,l-1}(p)$ can be obtained simply by

$$P_{l,l-1}(u) = \Phi_{l-1}(\Phi_l^{-1}(u)),$$
$$P_{l,l-1}(p) = \Psi_{l-1}(\Psi_l^{-1}(p)).$$

For details and properties one can consult [17; 22] and citations therein.

We solve the coupled system (1.19) by using an iterative method. Multigrid solvers for coupled velocity/pressure systems compute simultaneously the solution for both pressure and velocity and they are known to be ones of the best class of solvers for laminar Navier-Stokes equations (see [18; 26]). An iterative coupled solution of the linearized and discretized incompressible Navier-Stokes equations requires the approximate solution of sparse saddle point problems. In this multigrid approach the most suitable class of solvers is the Vanka-type smoothers. They can be considered as block Gauss-Seidel methods where one block consists of a small number of degrees of freedom (for details see [26; 17; 18]). The characteristic feature of this type of smoother is that in each smoothing step a large number of small linear systems of equations has to be solved. In the Vanca-type smoother, a block consists of all degrees of freedom which are connected to few neighboring elements. As shown in Figure 1.3 for conforming finite elements the block could consist of all the elements containing a pressure vertex or four pressure nodes , namely 21 velocity nodes (circles and squares) with one pressure node (square) or 16 velocity nodes (circles and squares) with four pressure nodes (squares) respectively. Thus, in the first case a relaxation step with this Vanca-type smoother consists of the iterative solution of the corresponding block of equations over all the pressure nodes. In the second case a relaxation step consists of the solution of the block of equations over all the elements where the velocity

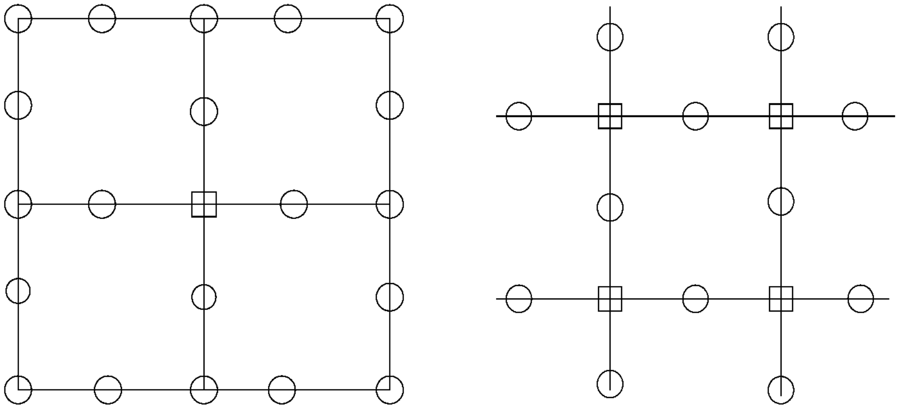

Fig. 1.3. Blocks of unknowns: $21V + 1P$ (on the left) and $16V + 4P$ (on the right).

and pressure variables are updated iteratively. Different blocks of unknowns can be solved including local constraints as they arise from the optimal control problem. For convergence and properties of this class of smoothers one can consult [26; 17; 18] and citations therein.

1.2.2 Boundary Control Test 1

We consider a unit square domain $\Omega = [0, 0.5] \times [0, 0.5]$ with boundary Γ as shown in Figure 1.2 on the left. Let $\widehat{\Omega}$ be $[0, 1] \times [0, 1]$. The boundary Γ consists of Γ_1, where homogeneous Dirichlet boundary conditions are applied, and Γ_c where the boundary control is applied. There are no Neumann boundary conditions and therefore Γ_2 is empty. The steady target velocity $\mathbf{U}$ for this test is given by

$$\begin{aligned} u(x, y) &= 2(1-x)^2(1-\cos(4\pi x))((1-y)(\cos(4\pi y)-1) \\ &\quad + 2\pi(1-y)^2 \sin(4\pi y)), \\ v(x, y) &= 2(1-y)^2(\cos(4\pi y)-1)((1-x)(\cos(4\pi x)-1) \\ &\quad + 2\pi(1-x)^2 \sin(4\pi x)). \end{aligned}$$

In Figure 1.4 we show the results for different values of the penalty parameter β for Reynolds numbers equal to 100 and rectangular isoparametric Taylor-Hood finite elements. On the top there is the extended solution $\widehat{u}$ over the extended domain $\widehat{\Omega}$ for $\beta = 10^{-3}$. The desired solution and the controlled solution (for asymptotic β) are shown in Figure 1.4 in the middle from the left to the right respectively. We note that the boundary control can achieve some matching of the desired flow if the normal and the tangential control are combined. This embedded method can handle the normal control in a relative straightforward manner, satisfies the compatibility constraint and improves the effectiveness of the control. In these computations $\Omega_1 = \Omega$ but a better matching can be reached if the controlled area Ω_1 is tuned. On the bottom of Figure 1.4

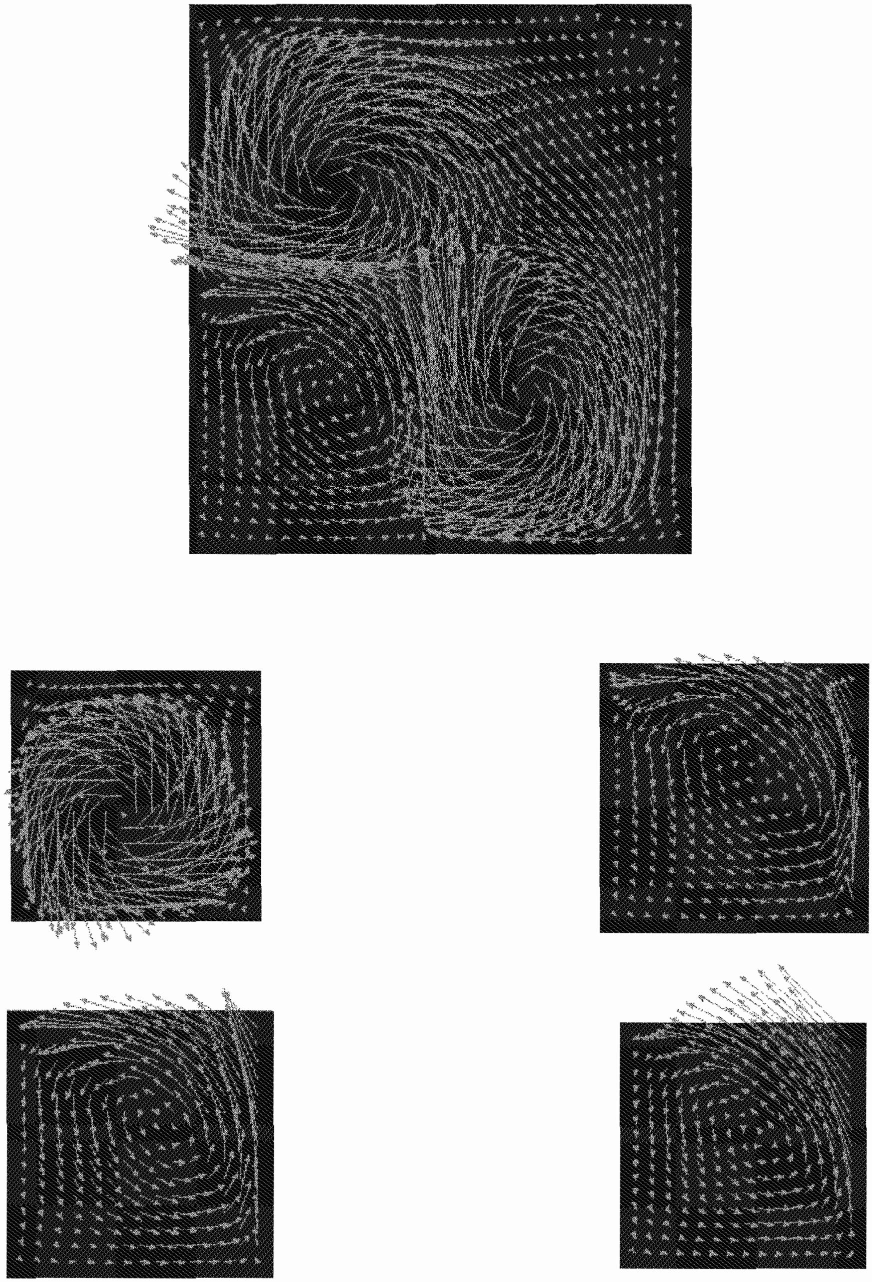

Fig. 1.4. Extended controlled flow (top) over $\widehat{\Omega} = [0,1] \times [0,1]$. Desired flow (central left) and controlled flow for $\beta = 1 \times 10^{-3}$ (central right), 1×10^{-2} (bottom left) and 1×10^{-1} (bottom right) over $\Omega = \Omega_1 = [0, 0.5] \times [0, 0.5]$.

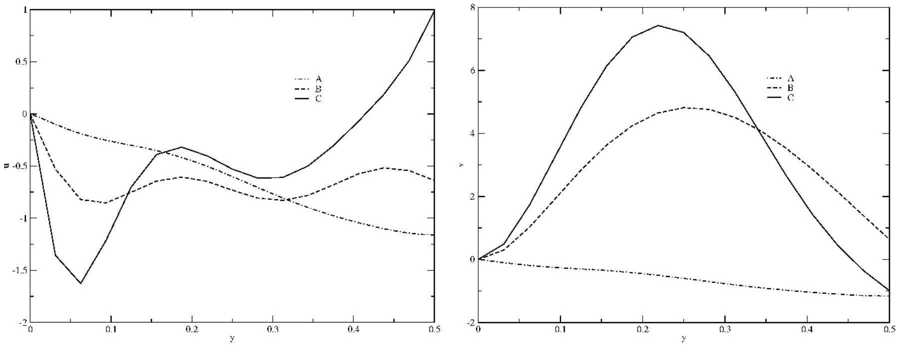

Fig. 1.5. Boundary control (u-component on the left and v-component on the right) on the vertical part of Γ_c for $\beta = 1 \times 10^{-1}$ (A), 1×10^{-2} (B) and 1×10^{-3} (C).

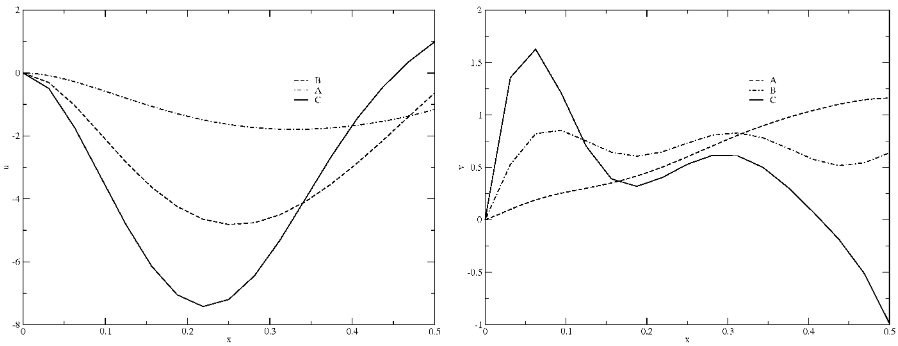

Fig. 1.6. Boundary control (u-component on the left and v-component on the right) on the horizontal part of Γ_c for $\beta = 1 \times 10^{-1}$ (A), 1×10^{-2} (B) and 1×10^{-3} (C).

we have the controlled solutions for different values of $\beta = 0.01$ (on the left) and $\beta = 0.1$ (on the right). The controlled boundary Γ_{ch} consists of a vertical and an horizontal part. Figure 1.5 shows the boundary control on the vertical part of Γ_c for $\beta = 1\times10^{-1}$ (A), 1×10^{-2} (B) and 1×10^{-3} (C). The u-component is shown on the left and the v-component on the right. In a similar way Figure 1.6 shows the u-component (on the left) and the v-component (on the right) of the horizontal part of the controlled boundary Γ_c for $\beta = 1 \times 10^{-1}$ (A), 1×10^{-2} (B) and 1×10^{-3} (C). We note that the controlled normal component of the boundary control may be positive and negative, namely there is injection and suction along the same portion of the boundary. If a standard non-embedded method is used the normal component of the control must satisfy the integral equation (1.4) and this may be numerically very challenging. Also this technique solves the corner point in a natural and straightforward manner while in the standard boundary control this point must be fixed by an artificial boundary condition which may limit the strength of the control.

In the second numerical experiment we would like to illustrate an example in which the boundary control can be efficiently applied to real situations. Suppose we have a velocity regulator as shown in Figure 1.1 on the left. The inflow over Γ_1 is assigned and we would like to control the fluid motion near to the output. By injection or suction along a portion of the boundary (for example Γ_c) it is possible to control accurately the velocity field. In order to model the problem we introduce, as shown in Figure 1.7 on the left, a L-shape domain with eight small cavities. The cavities are present in the real design and represent the area in which the fluid may be controlled. If a control is active in that area then we model such control as a boundary control, remove the cavity from the domain Ω and use it as a part of the extended domain. A very accurate study of this regulator can be done by taking into account all the seven cavities and the corresponding boundary controls but in this paper we investigate a simulation in which only the three parts of the boundary Γ_{1c}, Γ_{2c} and Γ_{3c} are controlled as shown in Figure 1.7 on the right. The desired velocity is a constant velocity field in the controlled area. The initial flow is a flow with parabolic velocity in Γ_1 with maximal velocity of $2.5m/s$. The Reynolds number of this initial velocity is 150 Reynolds with laminar motion everywhere. We compute the solution in two cases: constant horizontal target velocity of $0.5m/s$ (target case A) and $3.5m/s$ (target case B) in the controlled area. The controlled area, shown in Figure 1.8 on the left, is bounded by the line a and c. The vertical centerline of the controlled area is label by b. The stationary computations are performed with the penalty parameter β equal to 1000. In Figure 1.8 the controlled and desired u-component of the velocity are shown at $x = a$ (left), $x = b$ (center) and $x = c$ (right) for desired target case A and B. We note that the boundary suction and injection can control efficiently the average velocity to the target case A and B. In Figure 1.9-1.12 we see the controlled velocity for case A. In particular in Figure 1.9 the velocity field is shown in part of the domain Ω which is bounded on the right by the line c of the controlled area and from the left to the right of Figure 1.12 we have the boundary velocity over Γ_1, Γ_{2c} and Γ_{3c} respectively. In case A there is a strong suction in both boundary controls Γ_{1c} and Γ_{2c} in order to reduce the velocity in the controlled area and the boundary control in Γ_{3c} is relative small. In Figure 1.13 we see the velocity field for case B over boundary Γ_{1c} on the left, boundary Γ_{2c} in the center and boundary Γ_{3c} on the right.

In Figure 1.13 the u-component and the v-component of the velocity field are plotted as a function of the edge coordinate of the cavity. In this case there is suction in Γ_{1c} and injection in Γ_{2c} and Γ_{3c}. In case B the control in Γ_{3c} leads to a better matching in the desired velocity profile along c in the desired area close the upper boundary.

1.2.3 Boundary Control Test 2

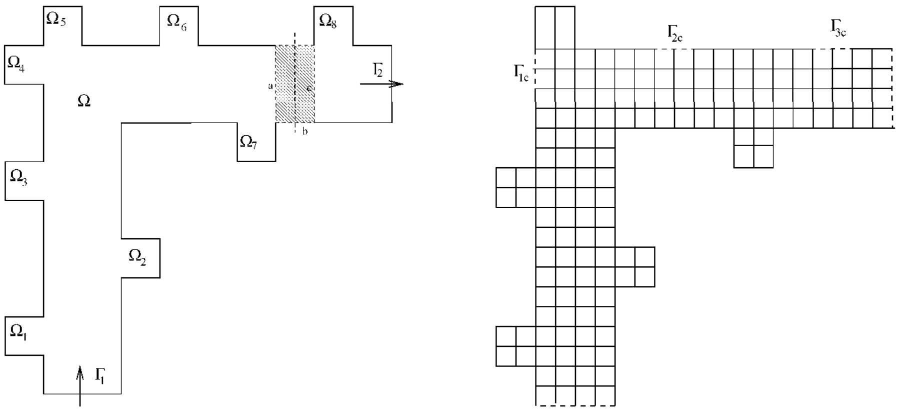

Fig. 1.7. Extended domain $\widehat{\Omega}$ (on the left) and domain Ω with boundary control over Γ_{1c}, Γ_{2c} and Γ_{3c} (on the right).

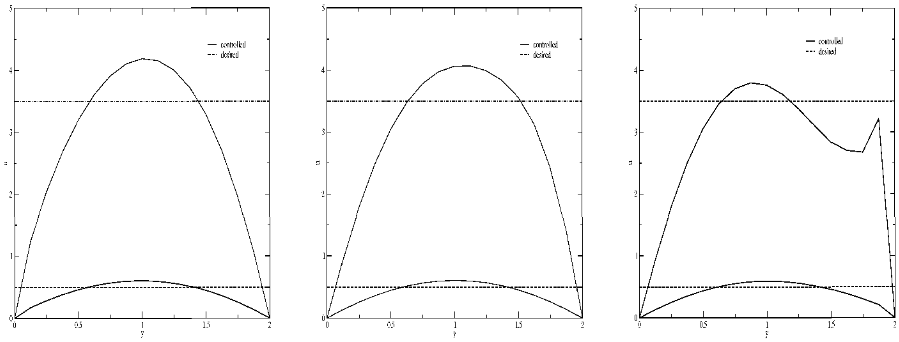

Fig. 1.8. Controlled and desired U-component of the velocity at $x = a$ (left), $x = b$ (center) and $x = c$ (right) in the controlled area for the desired target A and B.

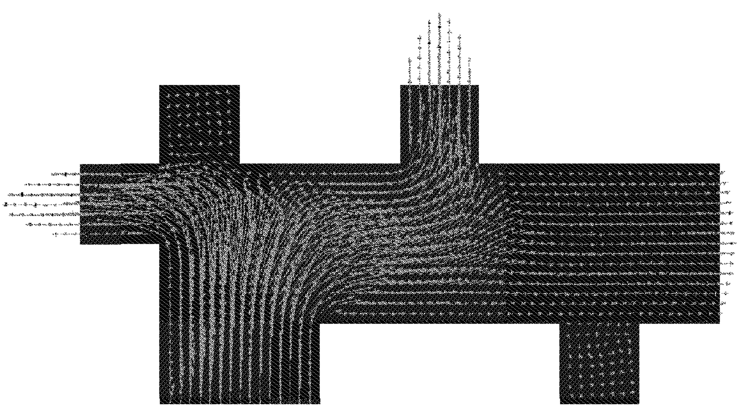

Fig. 1.9. Part of the velocity field for case A.

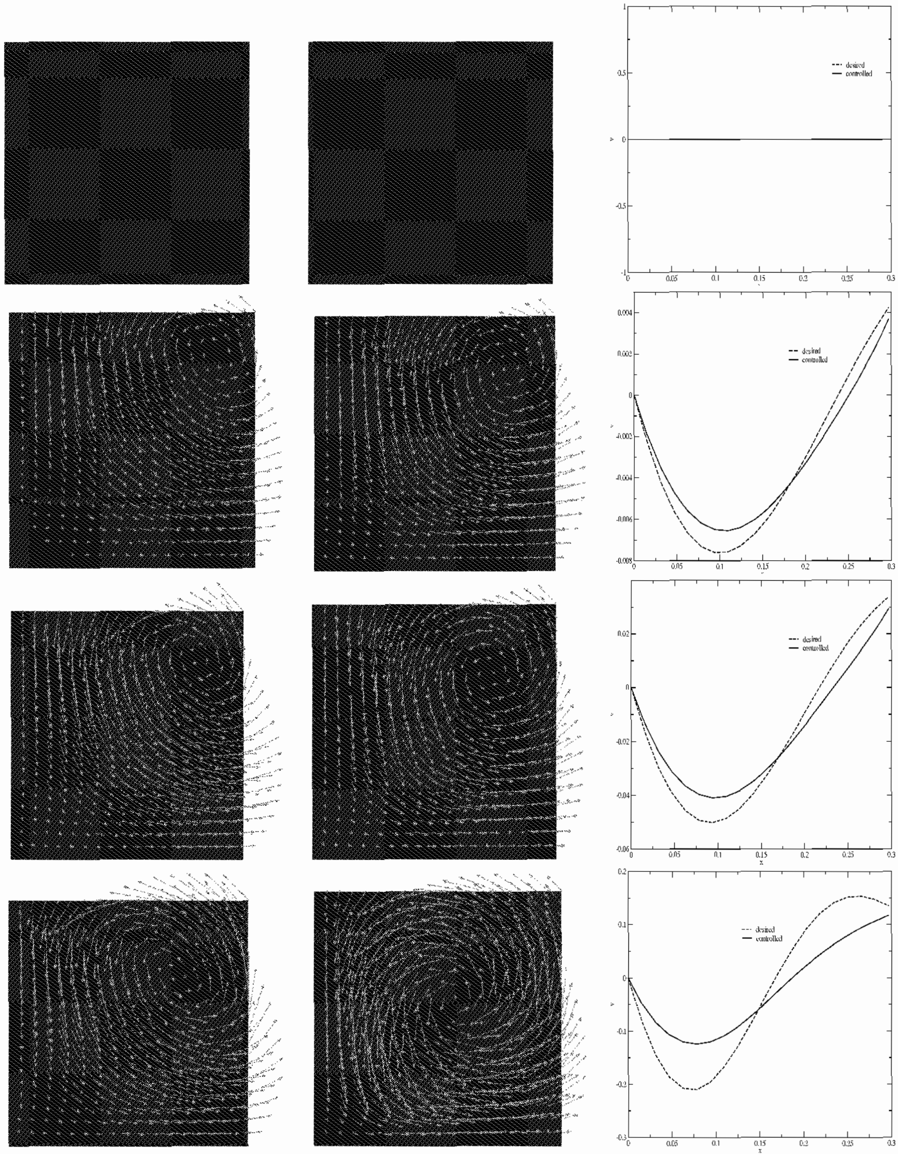

Fig. 1.10. Desired (left) and controlled (center) flow at different time $t = 0, 0.0125, 0.25$ and 0.75 from the top to the bottom. On the right the controlled and desired v-component along the x-axis at $y = 0.25$.

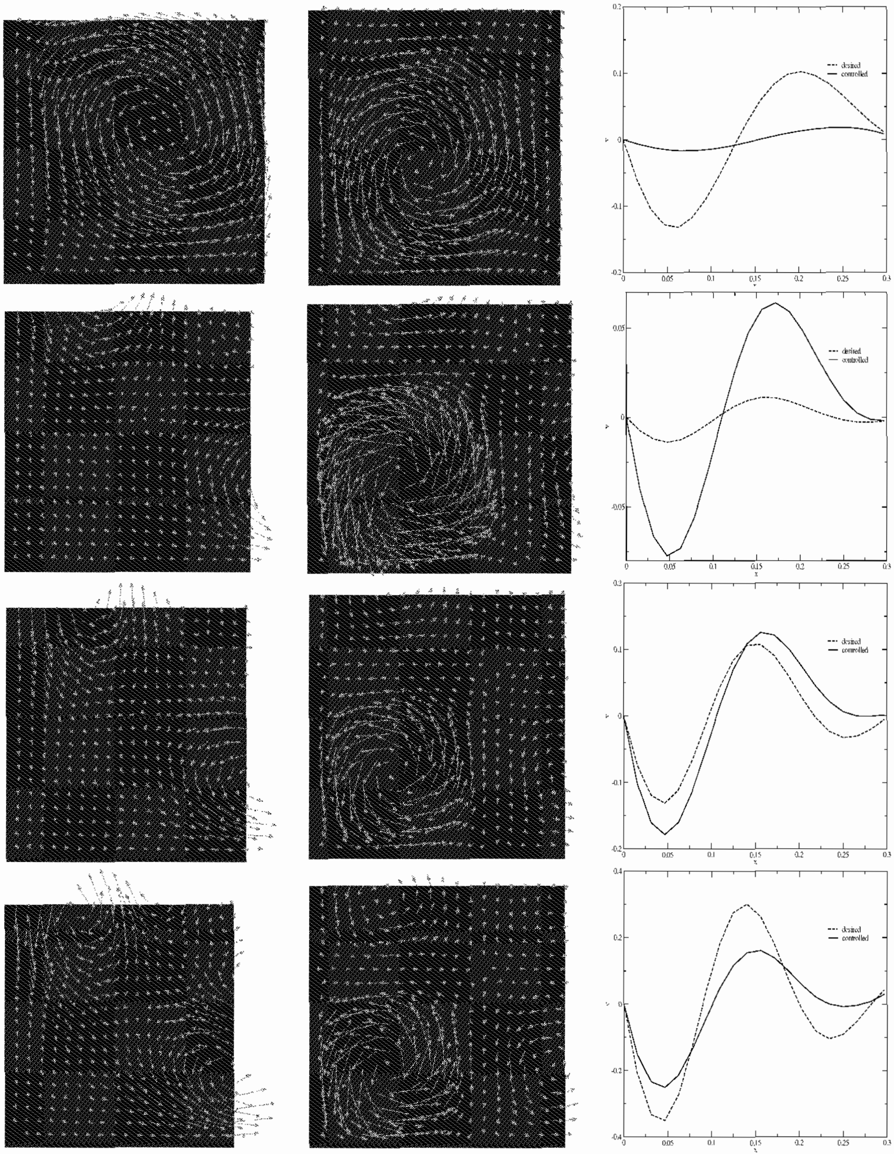

Fig. 1.11. Desired (left) and controlled (center) flow for different time $t = 1.5, 1.25, 1.325$ and 1.5 from the top to the bottom. On the right the controlled and desired v-component along the x-axis at $y = 0.25$.

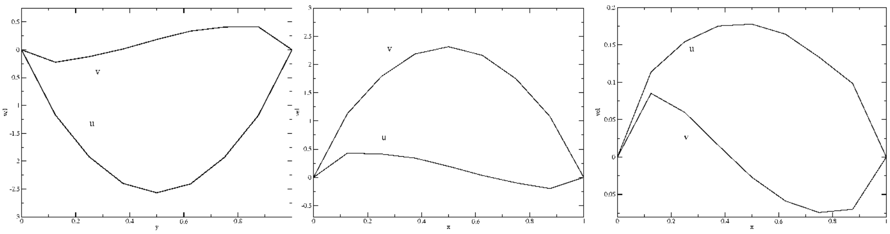

Fig. 1.12. Boundary control for case A. Boundary Γ_{1c} on the left, boundary Γ_{2c} in the middle and boundary Γ_{3c} on the right.

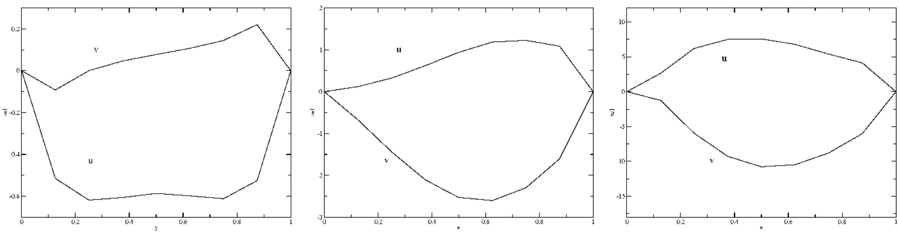

Fig. 1.13. Boundary control for case B. Boundary Γ_{1c} on the left, boundary Γ_{2c} on the center and boundary Γ_{3c} on the right.

1.3 Time Dependent Boundary Control Test

Now we test the proposed multigrid method with a time dependent boundary control problem. This problem reflects the desire to steer a candidate velocity field $\mathbf{u}$ to a given steady target velocity field $\mathbf{U}$ by appropriately controlling the velocity along a portion of the boundary of the flow domain. We consider a two-dimensional flow over a square domain $\Omega = [0, .35] \times [0, .35]$ with boundary Γ, control in $\Gamma_c \subset \Gamma$, homogeneous Dirichlet boundary condition in $\Gamma - \Gamma_c$ and extended domain $\widehat{\Omega} = [0,1] \times [0,1]$. The desired velocity $\mathbf{U} = (U, V)$ is given by

$$\phi(k,t,z) = (1 - \cos(2k\pi t z)) \times (1-z)^2 ,$$
$$U(t,x,y) = \frac{d}{dy}\left(\phi(k,t,x)\,\phi(k,t,y)\right),$$
$$V(t,x,y) = -\frac{d}{dx}\left(\phi(k,t,x)\,\phi(k,t,y)\right)$$

with $k = 2$. Since we can use the multigrid approach to solve the time dependent optimal control problem over a block of unknowns we consider piecewise continuous boundary control in time. We assume that the time interval $[0, T]$ is divided in m equal intervals of time $\Delta t = T/m$ and over each interval we seek a continuous boundary control. This allows to discretize the optimal control system over every interval Δt in a limited number of subinterval δt and solve exactly the system over all time-space domain by the multigrid technique proposed in the previous section. We remark that if ΔT is discretized by a single time step ($\delta t = \Delta t$) we recover the linear feedback control presented in [14]. The optimal boundary problem, by using the notation of the previous section, can be stated in the following way

find $\widehat{f} \in \mathbf{L}^2([0,T], \mathbf{L}^2(\widehat{\Omega} - \Omega))$ such that $(\widehat{u}, \widehat{p}, \widehat{\tau})$ minimizes the functional

$$\mathcal{J} = \frac{\alpha_0}{2} \int_0^T \int_{\Omega_1} |\mathbf{u} - \mathbf{U}|^2 \, d\mathbf{x} \, dt + \sum_{j=1}^{m} \frac{\alpha_j}{2} \int_{\Omega_2} |\mathbf{u}(T_j) - \mathbf{U}(T_j)|^2 \, d\mathbf{x} + \frac{\beta}{2} \int_0^T \int_{\widehat{\Omega}-\Omega} |\widehat{f}|^2 \, d\mathbf{x} \, dt$$

and satisfies

$$\begin{cases} \langle \widehat{u}_t, \widehat{v} \rangle + a(\widehat{u}, \widehat{v}) + c(\widehat{u}; \widehat{u}, \widehat{v}) + \langle \widehat{\tau}, \widehat{v} \rangle_{\widehat{\Gamma}} + b(\widehat{v}, p) = \langle \widehat{f}, \widehat{v} \rangle \\ \qquad \forall \widehat{v} \in \mathbf{H}^1_0(\widehat{\Omega}) \\ b(\widehat{u}, \widehat{q}) = 0, \quad \forall \widehat{q} \in L^2_0(\widehat{\Omega}) \\ \langle \widehat{u}, \widehat{s} \rangle_{\widehat{\Gamma}} = \langle \widehat{g}, \widehat{s} \rangle_{\widehat{\Gamma}}, \quad \forall \widehat{s} \in \mathbf{H}^{-1/2}(\widehat{\Gamma}) \end{cases} \tag{1.20}$$

with $\widehat{f} = \mathbf{f}$ over $[0,T] \times \Omega$. The term with the constant α_j is required if the adjoint function and therefore the control must not vanish at the end of the interval at the time T_j.

By using standard techniques (see for example [1; 8; 11; 12; 13]) we have that the optimal control solution must satisfy the following Navier-Stokes system over $[T_{j-1}, T_j]$

$$\begin{cases} \langle \widehat{u}_t, \widehat{v} \rangle + \nu a(\widehat{u}, \widehat{v}) + c(\widehat{u}; \widehat{u}, \widehat{v}) + b(\widehat{v}, \widehat{p}) = \langle \widehat{f}, \widehat{v} \rangle, \quad \forall \widehat{v} \in H^1_0(\widehat{\Omega}) \\ b(\widehat{u}, \widehat{q}) = 0, \quad \forall \widehat{q} \in L^2_0(\widehat{\Omega}) \\ (\widehat{u}, \widehat{s})_{\partial\widehat{\Omega}} = 0, \quad \forall \mathbf{s} \in H^{-1/2}(\partial\widehat{\Omega}) \\ \widehat{u}(T_{j-1}, \mathbf{x}) = \widehat{u}(T_{j-2}, \mathbf{x}), \quad \forall \mathbf{x} \in \widehat{\Omega} \end{cases}$$

the adjoint system over $[T_{j-1}, T_j]$

$$\begin{cases} -\langle \widehat{w}_t, \widehat{v} \rangle + \nu a(\widehat{w}, \widehat{v}) + c(\widehat{w}; \widehat{u}, \widehat{v}) + c(\widehat{u}; \widehat{w}, \widehat{v}) \\ \qquad + b(\widehat{v}, \widehat{\sigma}) = \alpha_0 (\mathbf{u} - \mathbf{U}, \widehat{v})_{\Omega_1}, \quad \forall \widehat{v} \in H^1_0(\widehat{\Omega}) \\ b(\widehat{w}, \widehat{q}) = 0, \quad \forall \widehat{q} \in L^2_0(\widehat{\Omega}) \\ \mathbf{w} = 0, \quad \forall \mathbf{x} \in \partial\widehat{\Omega} \\ \widehat{w}(T_j, \mathbf{x}) = \alpha_j (\widehat{u}(T_j) - \mathbf{U}(T_j)), \quad \forall \mathbf{x} \in \Omega_2 \end{cases}$$

for $j = 0, 1, \ldots, m$ and $\widehat{f} = \mathbf{f}$ over Ω and $\widehat{f} = \widehat{w}/\beta$ over $\widehat{\Omega} - \Omega$. The boundary control can be computed as $\mathbf{g} = \gamma_\Gamma \mathbf{u}$ with

$$\mathbf{g}_c = \gamma_{\Gamma_c} \widehat{u} \tag{1.21}$$

$\int_\Gamma \mathbf{g} \cdot \mathrm{n} \, d\Gamma = 0$. The optimality system for the boundary control can be computed in a very straightforward way if compared to other boundary control formulations.

In Figures 1.10-1.11 we show the desired (left) and the controlled (center) vector field for different time. All the figures are normalized with respect to the maximal velocity. From the left top to the bottom right of Figures 1.10-1.11 we have the velocity field at time $t = 0, 0.0125, 0.25, 0.75, 1.0, 1.25, 1.325$ and 1.5 respectively. The interval Δt is 0.025 with $\beta = 1000$ and $\alpha_j = 100$ with $j = 0, 1, \ldots$. Each interval has been divided in four time steps ($\delta = \Delta t/4$) and the complete optimality system solved with an exact method over all the time-space domain over the block of unknowns in Figure 1.3 on the right with a V-multigrid cycle. Since $\widehat{w}$ should not vanish at any time we set $\Omega_2 = [0, 0.5] \times [0, 0.5]$, namely $\Omega = \Omega_1 \subset \Omega_2 \subset \widehat{\Omega}$. On the right of Figures 1.10-1.11 the controlled and desired v-component along the x-axis at $y = 0.25$. It is clear that the matching is achieved essentially on the boundary and the boundary velocity cannot control the interior of the domain if the desired flow moves rapidly. However, this represents the optimum that can be achieved with the energy available.

1.4 Conclusions

We introduced an embedded method for boundary control which allows tracking and matching velocity field very efficiently. It is accurate and avoids the cumbersome regularizations of the standard boundary control. Also this methods allows to solve the problem for normal boundary control which must obey to the compatibility condition. A particular class of multigrid solvers is used in this paper to solve exactly the optimal control problem at the element level producing accurate and robust solutions. All this leads to improved computability and reliability for the numerical solution of steady and time dependent boundary control.

References

[1] F. Abergel and R. Temam, *On some control problems in fluid mechanics*, Theoretical and Computational Fluid Dynamics **1**, 1990, pp. 303-326
[2] R. Adams, *Sobolev Spaces*, Academic Press, New York,1975.
[3] G. Armugan and O. Pironneau, On the problem of riblets as a drag reduction device, *Optim. Control Appl. Meth.* **10** 1989, pp. 93–112.
[4] M. Berggren, *Numerical solution of a flow control problem: Vorticity reduction by dynamic boundary action* , Siam J. Sci. Comput., **19** (3), 1998